AD-A280 381

‖‖‖‖‖‖‖‖‖‖‖‖‖‖‖

ARRAY ELEMENT GAIN AND PHASE ESTIMATION IN THE PRESENCE OF INTERFERENCE (U)

by

Eric K.L. Hung

DTIC
ELECTE
JUN 1 7 1994
S
G
D

94-18816

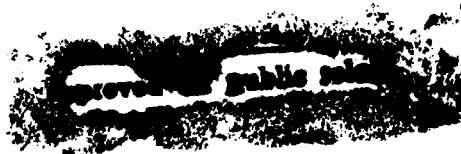‖‖‖‖‖‖‖‖‖‖‖‖‖‖‖

DTIC QUALITY INSPECTED 2

DEFENCE RESEARCH ESTABLISHMENT OTTAWA
REPORT N0. 1211

December 1993
Ottawa

94 6 16 088

ARRAY ELEMENT GAIN AND PHASE ESTIMATION IN THE PRESENCE OF INTERFERENCE (U)

by

Eric K.L. Hung
Surface Radar Section
Radar Division

Accesion For		
NTIS CRA&I		☒
DTIC TAB		☐
Unannounced		☐
Justification		
By		
Distribution /		
Availability Codes		
Dist	Avail and / or Special	
A-1		

DEFENCE RESEARCH ESTABLISHMENT OTTAWA
REPORT NO. 1211

December 1993
Ottawa

ABSTRACT

Presented is a method to estimate the element gains and phases of a sensor array when interfering signals, including specular multipath, are present. A movable calibration source is used. The element gains are derived from the relative output powers at the array elements. The element phases are obtained by transforming the array snapshots to make the source direction appear fixed and then maximizing a function constructed with the transformed snapshots.

Computer simulations produce highly accurate estimates of element gains and phases when the signal directions are known and the signal-to-noise ratio is reasonably high. When the directions are not known, the set of element phase estimates contains an additional component which produces a bias in direction estimates.

RÉSUMÉ

Nous présentons une méthode pour estimer les gains et les phases des éléments d'une antenne réseau en présence de brouillage incluant la réflexion spéculaire. Une source d'étalonnage amovible est utilisée. Les gains des éléments sont obtenus par les puissances relatives des sorties des éléments du réseau. Les phases sont obtenues en maximisant une fonction construite avec les vecteurs de données transformés de telle sorte que la direction de la source apparaisse fixe.

Quand la direction des signaux est connue et que le rapport Signal-sur-Bruit est raisonnablement élevé, nous obtenons des estimés très précis des gains et des phases des éléments par des simulations sur ordinateur. Par contre, quand les directions ne sont pas connues, l'ensemble des estimés des phases contient une composante supplémentaire qui produit un biais dans l'estimé des directions.

EXECUTIVE SUMMARY

Accurate calibration of a sensor array is essential when this array is used in direction-finding with modern high-resolution signal processing methods such as the MUSIC method.

This report discusses a new calibration technique that estimates the element gains and phases of an array when interfering signals, including specular multipath, are present. The technique uses a movable pilot source to generate the calibration data. Initially, the element gains are estimated from the output powers at the array elements. Next, a transformation is used to equalize the element gains and simultaneously fix the source direction in the data. Finally, the element phases are estimated by maximizing an objective function constructed with the transformed data.

Computer simulations show that the estimates of the element gains and phases are highly accurate if the calibration source directions are known and the signal-to-noise ratio at the array elements is 30 dB or higher.

TABLE OF CONTENT

LIST OF FIGURES

LIST OF TABLES

1.0 INTRODUCTION

Accurate calibration of a sensor array is essential if the outputs of this array are to be used in direction-finding with high-resolution methods such as the MUSIC method [1]. Otherwise, the ability of these methods to resolve signal directions would be degraded. A discussion of how sensor errors degrade the performance of the MUSIC method, for example, is given by Friedlander in [2].

Many techniques to calibrate a narrowband sensor array in the absence of specular multipath interference have been developed. They include those by Paulraj and Kailath [3], Friedlander and Weiss [4,5], Weiss, Willsky, and Levy [6], Brown, McClellan, and Holder [7,8], and Pierre and Kaveh [9]. In [3] to [6] the authors are concerned with the estimation of element gains and phases when mutual coupling among the array elements can be ignored. References [7] to [9] include the effects of mutual coupling.

The condition that specular multipath interference be absent is frequently not satisfied when the array has to be calibrated at the site of operation. This interference is unavoidable, for example, in the special case of an array antenna used to track low-flying targets over water, a high-frequency array used in direction-finding, and a sonar array for submarine detection.

This paper is concerned with the estimation of element gains and phases when specular multipath and other types of interference are present. A movable calibration source is used. Motion of the sensor array is allowed. Computer simulations show that the element gain and phase estimates are highly accurate if the calibration source directions are known and the signal-to-noise ratio (SNR) at the array elements is reasonably high.

The theory for this array calibration method are derived in Section 2. The procedure is described in Section 3. Some results of performance evaluations are presented in Section 4. The conclusions are given in Section 5.

1

2.0 THEORY

This estimation method is based on the use of a reasonably strong movable calibration source. The source motion is exploited to

(a)   Separate the estimation of element gains from the estimation of element phases,

(b)   Decorrelate the direct and indirect calibration signals at the array elements, and

(c)   Make each interfering signal source behave like a source spread out over a range of directions.

Some examples of source motion will be given later.

In the notation used, N denotes the number of array elements; $\underline{a}$, the vector $(a_1, a_2, \cdots, a_N)^T$; $\text{diag}\{\underline{b}\}$, the diagonal matrix $\text{diag}\{b_1, b_2, \cdots, b_N\}$; $\{g_1, g_2, \cdots, g_N\}$, the element gains; $\{\phi_1, \phi_2, \cdots, \phi_N\}$, the element phases; $|\cdot|$, the absolute value; and $E\{\cdot\}$, the expected value. Superscripts T and H represent the transpose and conjugate-transpose, respectively. The uniqueness conditions for the element gains and phases are defined as

$$g_1^2 + g_2^2 + \cdots + g_N^2 = N \tag{1}$$

and

$$\phi_1 + \phi_2 + \cdots + \phi_N = 0 \ . \tag{2}$$

The remainder of this section is organized as follows. Initially, the signal model and the estimation of element gains are described. Next, it is shown that there is a transformation which equalizes the element gains in the calibration data and simultaneously make the calibration source direction appear fixed. Finally, the estimation of element phases is discussed.

2.1 Signal Model

The array elements are isotropic. Mutual coupling is absent. Given that the calibration source direction is θ_c, a snapshot of the array element output is

$$\underline{x} = \alpha \ \underline{b}(\underline{g}, \underline{\phi}, \theta_c) + \text{interference} + \text{noise} \ , \tag{3}$$

where α is the signal amplitude and $\underline{b}(\underline{g}, \underline{\phi}, \theta_c)$ is the array manifold vector for θ_c. An array manifold vector for θ has the decomposition

$$\underline{b}(\underline{g}, \underline{\phi}, \theta) = \underline{G}(\underline{g}) \ \underline{T}(\underline{\phi}) \ \underline{a}(\theta) \ , \tag{4}$$

2

where

$$\underline{G}(\underline{g}) = \text{diag}\{\underline{g}\} \; , \tag{5}$$

$$\underline{T}(\underline{\phi}) = \text{diag}\{\underline{\tau}(\underline{\phi})\} \; , \tag{6}$$

vector $\underline{\tau}(\underline{\phi})$ is defined as

$$\tau_n(\underline{\phi}) = \exp[j\phi_n] \; , \qquad n=1,2,\cdots,N, \tag{7}$$

and $\underline{a}(\theta)$ is the array steering vector. For the sake of convenience, it will be assumed that the components of $\underline{a}(\theta)$ have unit magnitudes.

2.2   Estimation of Element Gains

By design, the direct signal from the calibration source is very strong compared with the signals from other sources. Specular multipath, if present, is effectively uncorrelated with the direct signal at the array elements. The element gains g_1 to g_N can therefore be derived from the average output powers at the array element. This calculation is straightforward and is given in the estimation procedure in Section III.

The direct and specular multipath signals are not correlated because their phase difference at each array element changes when the calibration source direction changes. Careful planning can make this difference change by thousands of degrees in the data.

2.3   Transformation for Calibration Data

The array manifold vector for the calibration source direction is given by (4) with $\theta=\theta_c$. A simple rearrangement yields

$$\underline{b}(\underline{g},\underline{\phi},\theta_c) = \underline{G}(\underline{g}) \; \underline{A}(\theta_c) \; \underline{\tau}(\underline{\phi}) \; , \tag{8}$$

where

$$\underline{A}(\theta_c) = \text{diag}\{\underline{a}(\theta_c)\}. \tag{9}$$

This rearrangement makes the phases of $\underline{a}(\theta_c)$ behave like element phases. It also makes $\underline{\tau}(\underline{\phi})$ behave like an array steering vector.

Let a transformation matrix, dependent on θ_c, be defined as

$$\underline{\Gamma}(\theta_c) = \underline{A}^{-1}(\theta_c) \; \underline{G}^{-1}(\underline{g}) \; . \tag{10}$$

Applied to the array manifold vector given by (4), it gives

$$\underline{\Gamma}(\theta_c) \; \underline{b}(\underline{g},\underline{\phi},\theta) = \underline{A}^{-1}(\theta_c) \; \underline{A}(\theta) \; \underline{\tau}(\underline{\phi})$$

$$= \underline{\tau}(\underline{\phi}) \; , \; \text{if } \theta=\theta_c \; . \tag{11}$$

Because $\underline{A}(\theta_c)$ and $\underline{A}(\theta)$ are diagonal and the diagonal elements have unit magnitudes, the transformed manifold vector can be treated as a vector with unit element gains, zero element phases, and a new steering direction determined by the right hand side of (11). For $\theta = \theta_c$, the new direction is determined by the phases of $\underline{r}(\underline{\phi})$ and is independent of θ_c.

Transformation matrix $\underline{\Gamma}(\theta_c)$ is designed for the calibration data in which each array snapshot has a different θ_c. It spreads out the power of each interfering source over a range of directions and simultaneously make the calibration signal behave like the strongest localized signal in the data.

2.4 Estimation of Element Phases

Matrix $\underline{\Gamma}(\theta_c)$ converts an array snapshot, given by (3), to

$$\underline{y} = \underline{\Gamma}(\theta_c) \ \underline{x}$$

$$= \alpha \ \underline{r}(\underline{\phi}) + \underline{z} \ , \qquad (12)$$

where $\underline{z}$ is the contribution from interference and noise. Because the calibration signal is uncorrelated with the interfering signals, the correlation matrix constructed with $\underline{y}$ is

$$\underline{R}_y = E\{\underline{y} \ \underline{y}^H\}$$

$$= |\alpha|^2 \ \underline{r}(\underline{\phi}) \ \underline{r}^H(\underline{\phi}) + \underline{R}_z \qquad (13)$$

where $\underline{R}_z = E\{\underline{z}\underline{z}^H\}$. In $\underline{R}_y$, the element gains are unity, the element phases are zero, and the array steering vector for calibration source direction is $\underline{r}(\underline{\phi})$.

Let the Capon method [10,11] be used to estimate the array output power for the source direction in $\underline{R}_y$. If $\hat{\underline{\phi}}$ is an estimate of $\underline{\phi}$ in this calculation, the power is

$$\mathcal{O}(\hat{\underline{\phi}}, \underline{R}_y) = \frac{1}{F(\hat{\underline{\phi}}, \underline{R}_y, \hat{\underline{\phi}})} \ , \qquad (14)$$

where

$$F(\underline{\phi}_a, \underline{R}_y, \underline{\phi}_b) = \underline{r}^H(\underline{\phi}_a) \ \underline{R}_y^{-1} \ \underline{r}(\underline{\phi}_b) \ . \qquad (15)$$

Because $\underline{R}_y$ is given by (13), application of the matrix inversion lemma leads to

$$\underline{R}_y^{-1} = \underline{R}_z^{-1} - \frac{|\alpha|^2 \ \underline{R}_z^{-1} \ \underline{r}(\underline{\phi}) \ \underline{r}^H(\underline{\phi}) \ \underline{R}_z^{-1}}{1 + |\alpha|^2 \ F(\underline{\phi}, \underline{R}_z, \underline{\phi})} \ . \qquad (16)$$

4

and

$$\mathcal{P}(\hat{\underline{\phi}},\underline{R}_y) = \frac{1 + |\alpha|^2 \, F(\underline{\phi},\underline{R}_z,\underline{\phi})}{F(\hat{\underline{\phi}},\underline{R}_z,\hat{\underline{\phi}}) + |\alpha|^2 \, G(\underline{\phi},\underline{R}_z,\hat{\underline{\phi}})} \, , \qquad (17)$$

with

$$G(\underline{\phi},\underline{R}_z,\hat{\underline{\phi}}) = F(\underline{\phi},\underline{R}_z,\underline{\phi}) \, F(\hat{\underline{\phi}},\underline{R}_z,\hat{\underline{\phi}}) - |F(\underline{\phi},\underline{R}_z,\hat{\underline{\phi}})|^2$$

$$= |\underline{q}|^2 \, |\hat{\underline{q}}|^2 - |\underline{q}^H \, \hat{\underline{q}}|^2 \, . \qquad (18)$$

The second line is obtained by noting that $\underline{R}_z^{-1}$ is the inverse of a non-singular correlation matrix when noise is present and that it has the decomposition

$$\underline{R}_z^{-1} = \underline{V} \, \underline{V}^H \, , \qquad (19)$$

where $\underline{V}$ is a non-singular matrix also. Vectors $\underline{q}$ and $\hat{\underline{q}}$ are defined as

$$\underline{q} = \underline{V} \, \underline{r}(\underline{\phi}) \qquad (20)$$

$$\hat{\underline{q}} = \underline{V} \, \underline{r}(\hat{\underline{\phi}}) \, . \qquad (21)$$

It follows from (2), (7), and Schwarz's inequality that

$$G(\underline{\phi},\underline{R}_z,\hat{\underline{\phi}}) \geq 0 \, . \qquad (22)$$

The equality sign holds if and only if $\hat{\underline{\phi}}=\underline{\phi}$.

The above results indicate that an estimate of $\underline{\phi}$ can be obtained by maximizing $\mathcal{P}(\hat{\underline{\phi}},\underline{R}_y)$ with respect to $\hat{\underline{\phi}}$, provided that the rate at which $F(\hat{\underline{\phi}},\underline{R}_z,\hat{\underline{\phi}})$ changes in the neighbourhood of $\underline{\phi}$ is small compared with that of $|\alpha|^2 G(\underline{\phi},\underline{R}_z,\hat{\underline{\phi}})$. Increasing $|\alpha|$ yields a more accurate estimate of $\underline{\phi}$. Making $F(\hat{\underline{\phi}},\underline{R}_z,\hat{\underline{\phi}})$ independent of $\hat{\underline{\phi}}$ yields $\hat{\underline{\phi}}=\underline{\phi}$.

3.0 ESTIMATION PROCEDURE

There are two variations of the calibration procedure: calibration source directions known, and calibration source directions not known. Both involve the maximization of an objective function with respect to the estimates of element phases. Some general properties of this function are also discussed.

3.1 Algorithm 1: Source Directions Known

Given a set of M array snapshots $\{\underline{x}_1, \underline{x}_2, \cdots, \underline{x}_M\}$ and corresponding calibration source directions $\{\theta_1, \theta_2, \cdots, \theta_M\}$, the estimation of array element gains and phases is as follows:

Step 1.

Estimate the average output powers at the array elements as

$$\hat{p}_n = \frac{|x_{1n}|^2 + |x_{2n}|^2 + \cdots + |x_{Mn}|^2}{M} , \tag{23}$$

where x_{mn} is the nth component of $\underline{x}_m$. Estimate the element gains as

$$\hat{g}_n = \sqrt{\frac{N \hat{p}_n}{\hat{p}_1 + \hat{p}_n + \cdots + \hat{p}_N}} , \tag{24}$$

Step 2.

Construct $\{\underline{y}_1, \underline{y}_2, \cdots, \underline{y}_M\}$, using (10) and (12). Use $\{\underline{x}_m, \underline{y}_m, \theta_m, \hat{\underline{g}}\}$ for $\{\underline{x}, \underline{y}, \theta_c, \underline{g}\}$.

Step 3.

Calculate

$$\hat{\underline{R}}_y = \frac{\underline{y}_1 \underline{y}_1^H + \underline{y}_2 \underline{y}_2^H + \cdots + \underline{y}_M \underline{y}_M^H}{M} \tag{25}$$

Step 4.

Define a function $\mathcal{P}(\underline{\phi}', \hat{\underline{R}}_y)$ with (14) and (15).

Step 5.

Identify $\hat{\underline{\phi}}$ as the $\underline{\phi}'$ which maximizes $\mathcal{P}(\underline{\phi}', \hat{\underline{R}}_y)$.
The implementation of Step 5 will be discussed later, after a discussion of the properties of $\mathcal{P}(\underline{\phi}', \hat{\underline{R}}_y)$.

6

3.2 Algorithm 2: Source Directions Not Known

In this method, the estimates of element gains are used to equalize the gains in the array snapshots. These modified snapshots are then used to estimate the calibration source directions. The procedure is as follows:

Step 1.

Step 1 of Algorithm 1.

Step 2A.

Construct a set of modified array snapshots $\{\underline{x}_1', \underline{x}_2', \cdots, \underline{x}_M'\}$ as

$$\underline{x}_m' = \underline{\underline{G}}^{-1}(\hat{\underline{R}}) \, \underline{x}_m, \qquad m=1,2,\cdots,M. \qquad (26)$$

Step 2B.

Estimate the calibration source directions from $\{\underline{x}_1', \underline{x}_2', \cdots, \underline{x}_M'\}$. Denote them by $\{\hat{\theta}_1, \hat{\theta}_2, \cdots, \hat{\theta}_M\}$.

Step 2C.

Construct $\{\underline{y}_1, \underline{y}_2, \cdots, \underline{y}_M\}$, using (10) and (12). Use $\{\underline{x}_m, \underline{y}_m, \hat{\theta}_m, \hat{\underline{g}}\}$ for $\{\underline{x}, \underline{y}, \theta_c, \underline{g}\}$.

Steps 3 to 5

Steps 3 to 5 of Algorithm 1.

The estimation of the source directions in Step 2B is highly dependent on the array and the interference conditions. Some examples will be given in Section IV.

3.3 Maximization of $\mathcal{P}(\underline{\phi}', \hat{\underline{R}}_y)$

A preliminary study of the properties of $\mathcal{P}(\underline{\phi}', \hat{\underline{R}}_y)$, as a function of $\underline{\phi}'$, has been made. Some notable results are listed below:

1. The element gain estimates are usually very accurate when the SNR at the array elements is 30 dB or larger and the number of array snapshots is reasonably large.

2. The function $\mathcal{P}(\underline{\phi}', \hat{\underline{R}}_y)$ is usually not unimodal. However, if the SNR is 30 dB or larger, the global maximum is usually the one closest to $\underline{\phi}$.

3. The finite precision in computer arithmetic introduces a small random error to the value of $\mathcal{P}(\underline{\phi}', \hat{\underline{R}}_y)$ calculated. This error is very difficult to handle in the maximization process unless

7

ϕ' always satisfies (2). The error also generates many false maxima in the neighbourhood of each true maximum. The density and peak values of these false maxima generally increase as the Euclidean distance from the true maximum decreases or as the value of the true maximum increases.

Because of the above observations, Step 5 in the estimation procedure is implemented in the following manner:

Step 5A.

Initialize the components of ϕ' as samples of a random variate uniformly distributed in the range [-90,90] degrees. Use hill-climbing with random searches at each local maximum in the maximization. Modify one component of ϕ' at a time. Impose (2) on the modified ϕ' before calculating $\mathcal{P}(\phi',\hat{R}_y)$.

Step 5B.

Repeat the Step 5A K times, using a large K. Denote the maximum positions and values by $\{\phi_k, \mathcal{P}_k; k=1,2,\cdots,K\}$, respectively. Identify the largest $\mathcal{P}_k$ as the value at the global maximum and denote it by $\mathcal{P}$. Identify the corresponding ϕ_k as the estimate $\hat{\phi}$.

4 PERFORMANCE EVALUATION

Four examples have been designed to evaluate the performance of the array calibration method. The scenarios are the four combinations of

(a) Calibration source directions known
     or
     Calibration source directions not known, and

(b) Number of interfering sources larger than number of array elements
     or
     A strong specular multipath interference present.

The true element gains in the simulations are unity and the components of $\underline{\phi}$ are samples of a Gaussian variate with zero mean and eight degrees standard deviation. Five hundred (K=500) sets of $\{\underline{\phi}_k, \mathcal{P}_k\}$ are calculated in Step 5B in each example.

It is not necessary to evaluate the calibration method with true element gains other than unity. As long as these gains are close to unity, the percentage errors in the estimates are insensitive to the true values. This property can be verified by noting that the replacement of $\underline{g}=(1,1,\cdots,1)^T$ by $\underline{g}=\underline{\beta}$, leads to the replacement of $\underline{x}_m$ by $\text{diag}\{\underline{\beta}\}\underline{x}_m$ and $\hat{g}_n$ in (24) by $\kappa\beta_n\hat{g}_n$. The scaling factor κ is close to unity if the components of $\underline{\beta}$ are also close to unity.

In the presentation of results, the maximum $\mathcal{P}_k$ relative to the largest maximum $\mathcal{P}$ is

$$\rho_k = \frac{\mathcal{P}_k}{\mathcal{P}} \; ; \tag{27}$$

the root mean square (RMS) error in $\underline{\phi}_k$ is

$$\epsilon_k = \frac{|\underline{\phi}_k - \underline{\phi}|}{\sqrt{N}} \; ; \tag{28}$$

the distance between $\underline{\phi}_j$ and $\underline{\phi}_k$ is $|\underline{\phi}_j - \underline{\phi}_k|$; and direction in beamwidth is $N d \sin\theta$, where d is the element spacing in wavelengths.

Example 1.

In this example the calibration source directions are known and the number of interfering sources is larger than the number of array elements. The array is shown in Fig. 1. It has eight elements (N=8) spaced at a distance of half a wavelength (d=0.5 wavelength). The signal scenario is shown in Fig. 2. A calibration source giving

9

a 30 dB SNR at the array elements is used. It moves in direction from -6.28 to 6.28 degrees and is represented by a horizontal line with arrow heads at the ends. Ten 10-dB SNR interfering signals, represented by vertical arrows, are present. Four are located at (-41,-19,0,19) degrees and six are in the range [33,50] degrees. They are uncorrelated with each other and with the calibration signal. Four hundred (M=400) array snapshots are generated. Algorithm 1 for known calibration source directions is used.
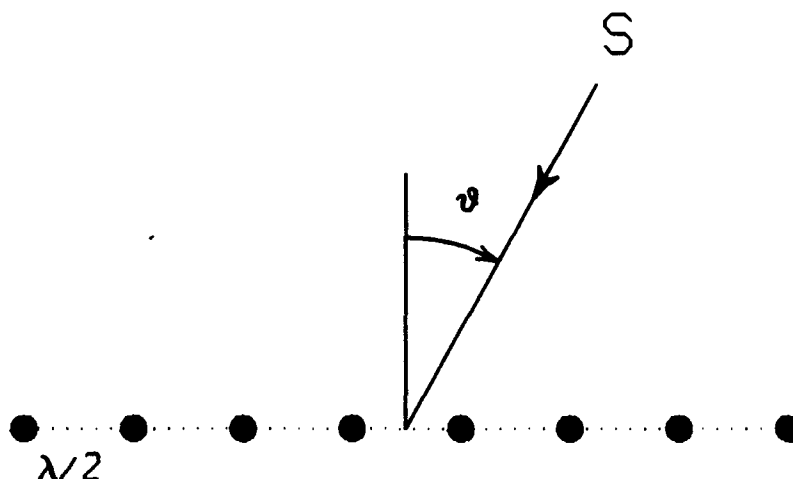

Fig. 1   Array Configuration in Examples 1 and 2.

The true and estimated values of element gains and phases are shown in Table 1. The errors in gain estimates are 1.5% or less and the errors in phase estimates are 0.2 degree or less. Out of the 500 maximisation runs in element phase estimation, 481 terminate in the region of the global maximum. Each produces a maximum value $\mathcal{P}_k$ between 1035.03 and 1037.01 σ^2, where σ^2 is the white noise power. The positions of the ten largest maxima are separated from each other and from the true ϕ by less than 0.4 degree. The other 19 runs terminate at positions with $\mathcal{P}_k$ between 9.16 and 12.01 σ^2. These positions are separated from each other and from the true ϕ by at least 10 degrees. The distribution of relative power is shown in Fig. 3, where the horizontal line between $\rho=0.012$ and 0.998 reflects the absence of any $\mathcal{P}_k$ between 12.01 and 1035.03 σ^2. The dependence of ϵ_k on ρ_k in the region of the global maximum is shown in Fig. 4. Here, the RMS error ϵ_k is less than 0.25 degree for ρ_k larger than 0.9990.
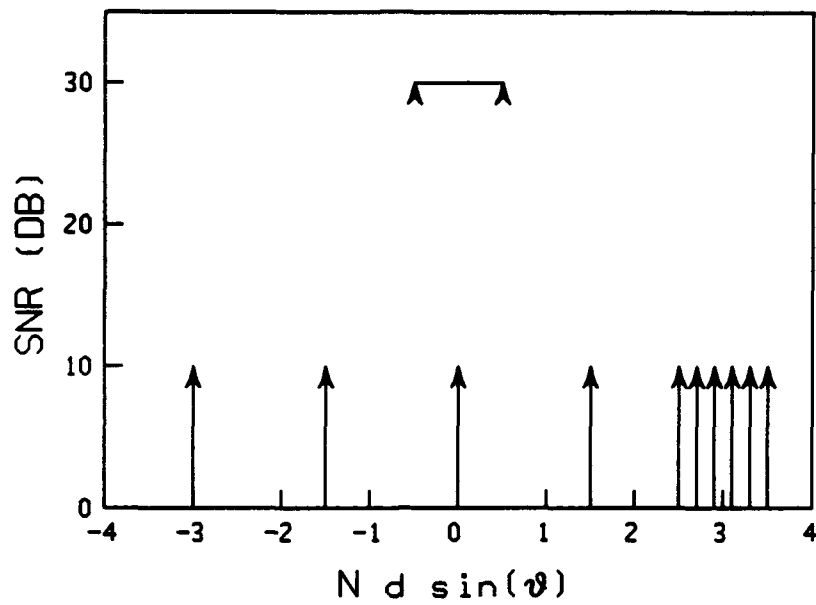
10

Fig. 2   Signals in Examples 1 and 3.

	GAIN		PHASE (DEG)	
n	g	$\hat{g}$	ϕ	$\hat{\phi}$
1	1.000	1.010	-6.8	-6.7
2	1.000	1.003	-1.9	-1.9
3	1.000	0.993	7.5	7.4
4	1.000	0.985	2.7	2.7
5	1.000	0.992	-7.1	-7.1
6	1.000	0.998	7.2	7.0
7	1.000	1.008	3.3	3.4
8	1.000	1.010	-4.9	-4.7

Table 1:   True and estimated values of element gains and phases in Example 1.
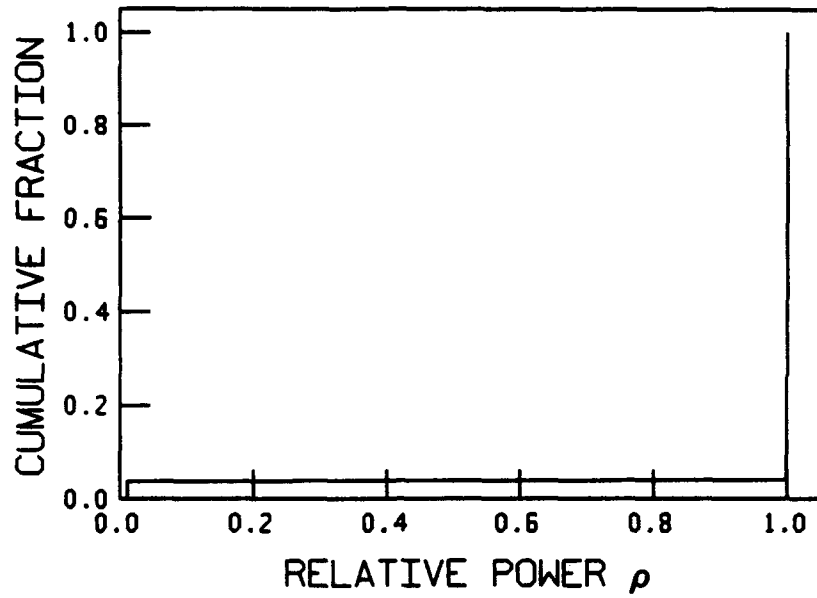
11

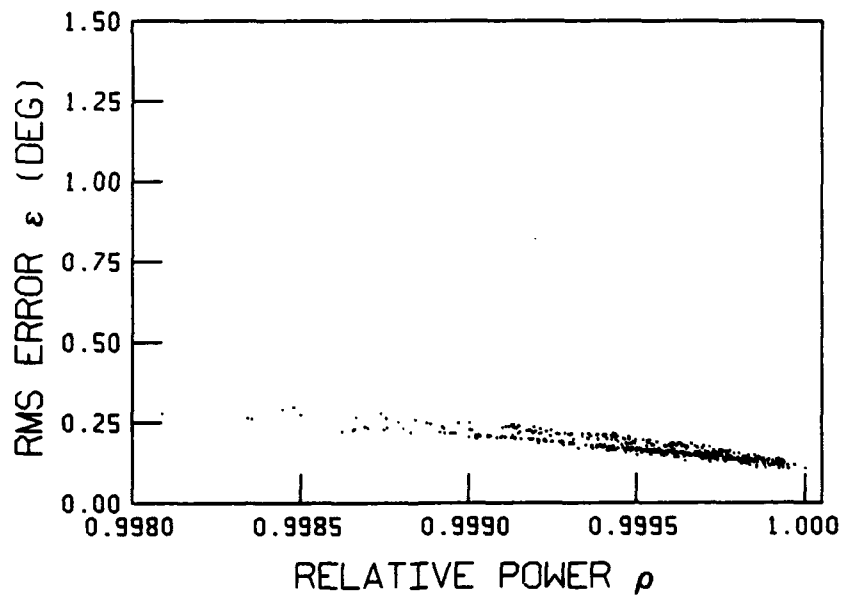Fig. 3 Distribution of output powers in Example 1. Calibration source directions are know.

Fig. 4 Dependence of ϵ_k on ρ_k in the global maximum region in Example 1. Calibration source directions are known.

Example 2

In this example the calibration source directions are known and a strong specular multipath interference is present. The array is a radar antenna used to track low-flying targets over water. It operates at 10 GHz, has eight isotropic elements spaced at a vertical distance of 12.5 cm (d=4.17 wavelengths), and is centred at a height of 15 m. The arrangements for measuring calibration data are shown in Fig. 5. An active source is mounted on a tower 500 m in front of the array. It moves up in equal steps from 10 to 25 m. A flat earth model for the specular multipath is used. The reflection coefficient at the surface is -1, corresponding to 0 dB power attenuation and 180 degrees phase change. The noise is white, and the SNR at the array elements is 30 dB. Four hundred array snapshots are generated. Algorithm 1 is used.
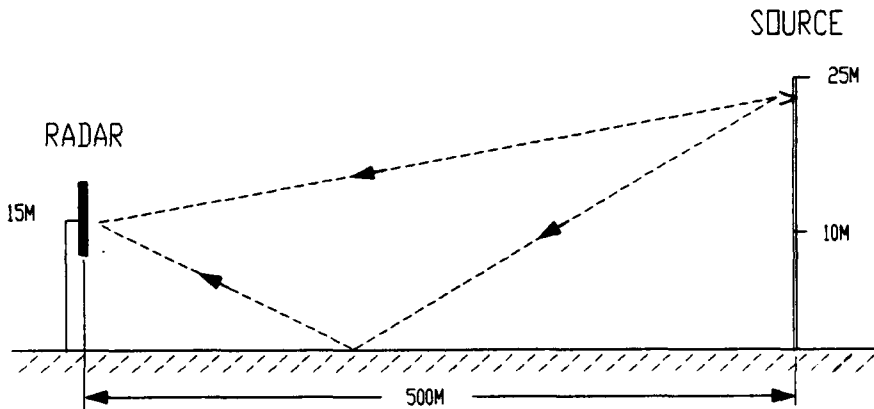

Fig. 5 Arrangements for calibration data measurement in Example 2 and 4.

The true and estimated element gains and phases are shown in Table 2, where the errors in gain and phase estimates do not exceed 0.4% and 0.3 degree, respectively. Out of the 500 maximization runs in phase estimation, 238 terminate in the region of global maximum and have $\mathcal{P}_k$ between 999.51 and 1000.61 σ^2. The ten positions with the largest maxima are separated from each other and from ϕ by less than 0.7 degree. The distribution of relative power ρ_k is shown in Fig. 6 and the dependence of RMS error ϵ_k on ρ_k in the region of global maximum is shown in Fig. 7.
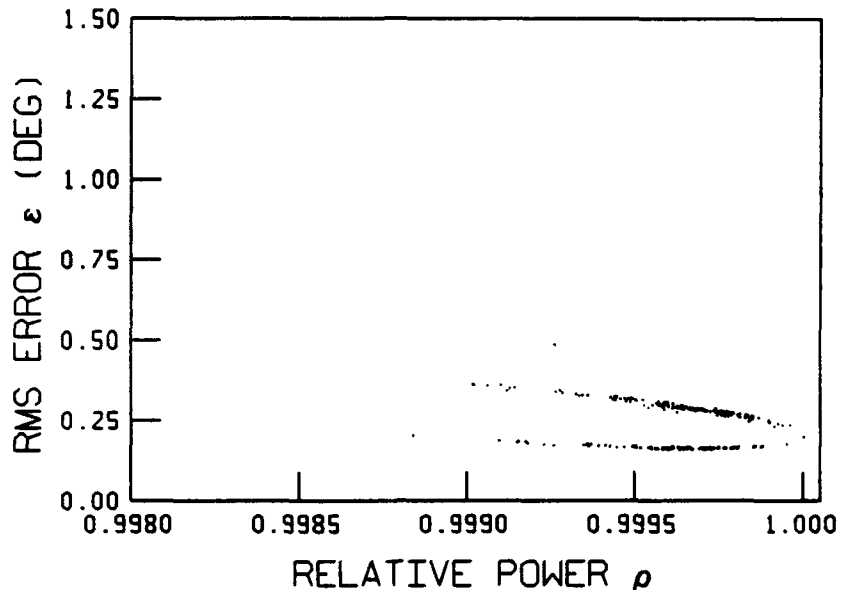
13

Fig. 7 Dependence of ϵ_k on ρ_k in the global maximum region in Example 3. Calibration source directions are known.

In this example, the direct and specular multipath signals are equally strong at the array elements. The peak values of some local maxima are larger than $420\sigma^2$. As the calibration source moves up from 10 to 25 m, the angular separation between the direct and reflected signals increases from 2.29 to 5.73 degrees (1.52 to 3.81 beamwidths), and their phase difference at the array centre increases from 7020 to 17820 degrees.

Example 3

Here, the calibration source directions are not known and the number of interfering sources is larger than the number of array elements. The array, signal scenario, and calibration data are identical to those in Example 1. Algorithm 2 is used.

The calculation of $\hat{\theta}_m$ in Step 2B is as follows. Initially, $\underline{x}_m'$ is used with the root variant of the modified covariance method [12] and a third order linear prediction filter to produce three candidate source direction estimates. Next, the power associated with each estimate is calculated. Finally, the estimate with the largest power is identified as $\hat{\theta}_m$.

In the results, the element gain estimates are, as expected, identical to those of Example 1. The distribution of relative power ρ_k is essentially the same as Fig. 3. The dependence of ϵ_k on ρ_k in

15

the region of global maximum is shown in Fig. 8. Here, RMS error ϵ_k is less than 0.75 degree for ρ_k larger than 0.9990. The ten largest maxima are separated from each other by less than 0.3 degree. Their distances from $\underline{\phi}$ are slightly less than 2.0 degrees.
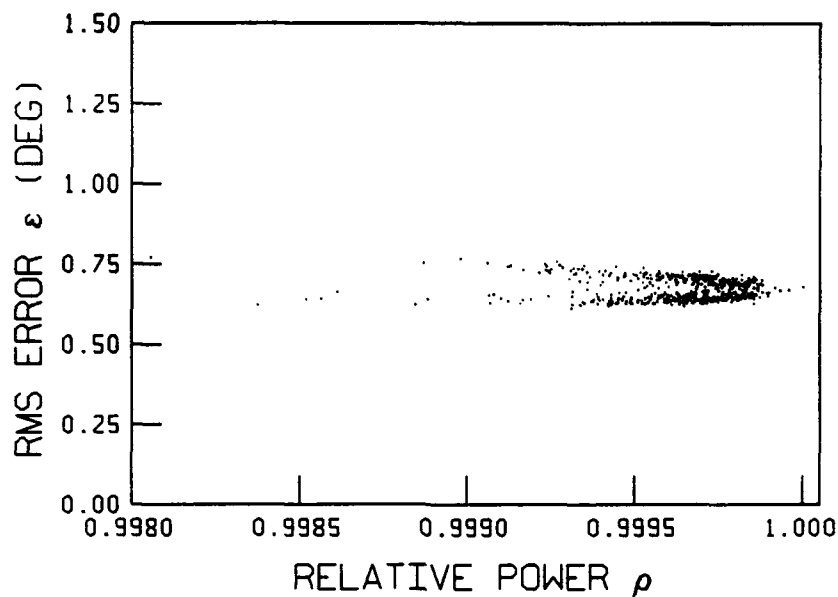

Fig. 8 Dependence of ϵ_k on ρ_k in the global maximum region in Example 2. Calibration source directions are estimated.

The estimate $\hat{\underline{\phi}}$ is given in Column 3 of Table 3. Its deviation from the true $\underline{\phi}$ in Column 2 is the $\underline{\delta}$ in Column 4. This deviation is decomposed into a linear component $\underline{\delta}_L$ in Column 5 and a random component $\underline{\delta}_R$ in Column 6, using the least squares linear curve fitting method. The linear component decreases in steps of 0.291 degree down the table. The random component is 0.2 degree or less in magnitude.

The linear component δ_L produces a bias in signal direction estimates when $\hat{\underline{\phi}}$ is used in array calibration. This bias comes from the errors in estimating the calibration source directions.

	PHASE (DEG)				
n	ϕ	$\hat{\phi}$	δ	δ_L	δ_R
1	-6.8	-5.6	1.2	1.0	0.2
2	-1.9	-1.3	0.6	0.7	-0.1
3	7.5	7.8	0.4	0.4	-0.1
4	2.7	2.9	0.1	0.1	0.0
5	-7.1	-7.2	-0.1	-0.1	0.0
6	7.2	6.5	-0.7	-0.4	-0.2
7	3.3	2.6	-0.7	-0.7	0.1
8	-4.9	-5.8	-0.9	-1.0	0.1

Table 3: True element phases ϕ, estimated phases $\hat{\phi}$, errors in estimates δ, linear component of errors δ_L, and random component of errors δ_R in Example 3.

Example 4

Here, the calibration source directions are not known and a strong specular multipath is present. The array, signal scenario, and calibration data are identical to those in Example 2. Algorithm 2 is used.

The calculation of $\hat{\theta}_m$ in Step 2B is as follows. Firstly, the x_m' is used to calculate three candidate direction estimates. Next, the power associated with each estimate is calculated and the estimate with the smallest power deleted. Finally, the remaining estimate with a larger elevation is identified as $\hat{\theta}_m$.

The element phase estimates are given in Column 3 of Table 4. The errors have a linear component which changes by 0.535 degree between adjacent elements. When this component is removed, the error magnitudes are 0.3 degree or less. The distribution of relative power ρ_k is essentially the same as Fig. 7. The dependence of ϵ_k on ρ_k in the region of global maximum is shown in Fig. 9, where the RMS error ϵ_k is less than 1.5 degree for ρ_k larger than 0.9990. The ten largest maxima are separated from each other by less than 0.9 degree and their distances from ϕ are less than 4.0 degree.

17

	PHASE (DEG)				
n	ϕ	$\hat{\phi}$	δ	δ_L	δ_R
1	-6.8	-5.0	1.8	1.9	0.0
2	-1.9	-0.9	1.1	1.3	-0.3
3	7.5	8.4	0.9	0.8	0.1
4	2.7	3.1	0.3	0.3	0.0
5	-7.1	-7.1	0.0	-0.3	0.3
6	7.2	6.6	-0.6	-0.8	0.2
7	3.3	1.9	-1.4	-1.3	-0.1
8	-4.9	-7.0	-2.1	-1.9	-0.2

Table 4: True element phases ϕ, estimated phases $\hat{\phi}$, errors in estimates δ, linear component of errors δ_L, and random component of errors δ_R in Example 4.

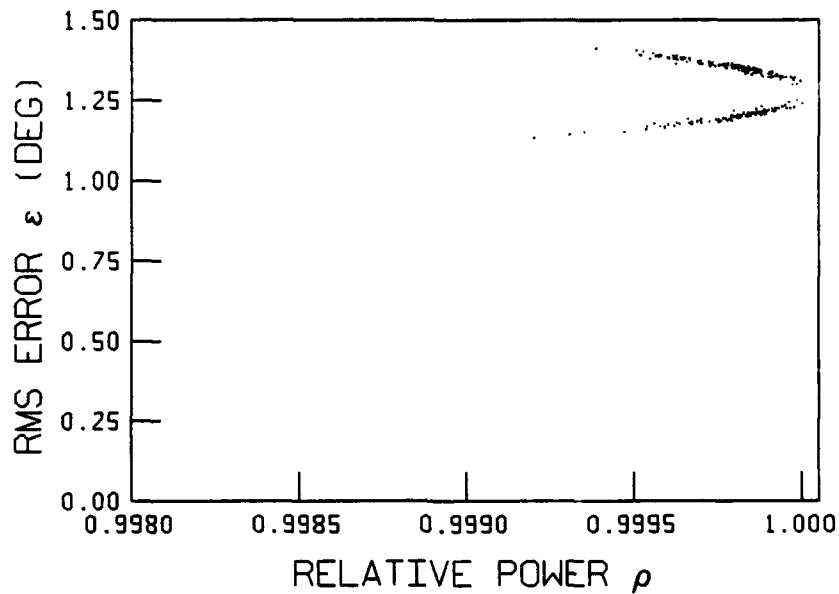Fig. 9 Dependence of ϵ_k on ρ_k in the global maximum region in Example 4. Calibration source directions are estimated.

5 CONCLUSIONS

A method which uses a movable calibration source to estimate the element gains and phases of a sensor array has been described. This method is highly tolerant to interference, including specular multipath. The number of interfering sources also need not be known or be smaller than the number of array elements. Computer simulations with reasonably strong calibration signals produce highly accurate gain and phase estimates when the source directions are known. When the directions are not known, the set of element phase estimates contains an additional component which corresponds to a bias in direction estimates.

This method has many applications. One example is the calibration of a high-frequency array used in direction-finding. The method accounts for the presence of other signal sources as well as the indirect signals from the ionosphere and other reflectors. Another example is the calibration of a sonar array in the ocean. The method accounts for the surface and bottom reflections as well as the interfering signals from ships and marine life. A third example is the calibration of an array antenna used to track low-flying targets over water. The method accounts for the specular reflection at the water surface.

The calibration method has the limitation that mutual coupling among the array elements is absent. It appears that there is no simple modification which can take this coupling into consideration.

19

REFERENCES

1. R.O. Schmidt, "Multiple Emitter Location and Signal Parameter Estimation", IEEE Trans. Antennas and Progag., vol. AP-34, pp. 276-280, March 1986.

2. B. Friedlander, "A Sensitivity Analysis of the MUSIC Algorithm", IEEE Transactions on Acoustics, Speech, and Signal Processing, Vol. 38, pp. 1740-1751, October 1990.

3. A. Paulraj and T. Kailath, "Direction of Arrival Estimation by Eigenstructure Methods with Unknown Sensor Gain and Phase", ICASSP 1985, Tampa, U.S.A., pp. 640-643, March 1985.

4. B. Friedlander and A.J. Weiss, 'Eigenstructure Methods for Direction Finding with Sensor Gain and Phase Uncertainties,' ICASSP 1988, New York, U.S.A., pp. 2681-2684, April 1988.

5. A.J. Weiss and B. Frielander, 'Eigenstructure Methods for Direction Finding with Sensor Gain and Phase Uncertainties', Circuits and Systems and Signal Processing, Vol. 9, No. 3, pp. 271-300, 1990.

6. A.J. Weiss, A.S. Willsky, and B.C. Levy, 'Eigenstructure Approach for Array Processing with Unknown Intensity Coefficients,' IEEE Transactions on Acoustics, Speech, and Signal Processing, Vol. 36, October 1988.

7. G.C. Brown, J.H. McClellan, and E.J. Holder, "A Phased Array Calibration Technique using Eigenstructure Methods", IEEE 1990 International Radar Conference, Arlington, U.S.A., pp. 304-307, May 1990.

8. G.C. Brown, J.H. McClellan, and E.J. Holder, "Eigenstructure Approach for Array Processing and Calibration with General Phase and Gain Perturbations", ICASSP 91, Toronto, Canada, pp. 3037-3040, May 1991.

9. J. Pierre and M. Kaveh, "Experimental Performance of Calibration and Direction-Finding Algorithms", ICASSP 91, Toronto, Canada, pp. 1365-1368, May 1991.

10. J. Capon, "High-Resolution Frequency-Wavenumber Spectrum Analysis", Proceedings of the IEEE, vol. 57, pp. 1408-1418, August 1969.

11. R.T. Lacoss, "Data Adaptive Spectral Analysis Methods", Geophysics, Vol. 36, pp. 661-675, August 1971.

12. See, for example, Chapter 8 in S.L. Marple, Jr., Digital Spectral Analysis With Applications, Prentice-Hall, Englewood Cliffs, New Jersey 07632, U.S.A., 1987.

DOCUMENT CONTROL DATA

(Security classification of title, body of abstract and indexing annotation must be entered when the overall document is classified)

1. ORIGINATOR (the name and address of the organization preparing the document. Organizations for whom the document was prepared, e.g. Establishment sponsoring a contractor's report, or tasking agency, are entered in section 8.) Department of National Defence Defence Research Establishment Ottawa Shirleys Bay, Ottawa, Ontario, Canada K1A 0K2	2. SECURITY CLASSIFICATION (overall security classification of the document. including special warning terms if applicable) UNCLASSIFIED

3. TITLE (the complete document title as indicated on the title page. Its classification should be indicated by the appropriate abbreviation (S,C or U) in parentheses after the title.)

Array Element Gain and Phase Estimation in the Presence of Interference (U)

4. AUTHORS (Last name, first name, middle initial)

Eric K.L. Hung

5. DATE OF PUBLICATION (month and year of publication of document) December 1993	6a. NO. OF PAGES (total containing information. Include Annexes, Appendices, etc.) 22	6b. NO. OF REFS (total cited in document) 12

7. DESCRIPTIVE NOTES (the category of the document, e.g. technical report, technical note or memorandum. If appropriate, enter the type of report, e.g. interim, progress, summary, annual or final. Give the inclusive dates when a specific reporting period is covered.)

Technical Report

8. SPONSORING ACTIVITY (the name of the department project office or laboratory sponsoring the research and development. Include the address.)

Department of National Defence
Defence Research Establishment Ottawa
Shirleys Bay, Ottawa, Ontario, Canada   K1A 0K2

9a. PROJECT OR GRANT NO. (if appropriate, the applicable research and development project or grant number under which the document was written. Please specify whether project or grant) 041ZW	9b. CONTRACT NO. (if appropriate, the applicable number under which the document was written)

10a. ORIGINATOR'S DOCUMENT NUMBER (the official document number by which the document is identified by the originating activity. This number must be unique to this document.) DREO REPORT 1211	10b. OTHER DOCUMENT NOS. (Any other numbers which may be assigned this document either by the originator or by the sponsor)

11. DOCUMENT AVAILABILITY (any limitations on further dissemination of the document, other than those imposed by security classification)

(X) Unlimited distribution
( ) Distribution limited to defence departments and defence contractors; further distribution only as approved
( ) Distribution limited to defence departments and Canadian defence contractors; further distribution only as approved
( ) Distribution limited to government departments and agencies; further distribution only as approved
( ) Distribution limited to defence departments; further distribution only as approved
( ) Other (please specify):

12. DOCUMENT ANNOUNCEMENT (any limitation to the bibliographic announcement of this document. This will normally correspond to the Document Availability (11). However, where further distribution (beyond the audience specified in 11) is possible, a wider announcement audience may be selected.)

13. ABSTRACT (a brief and factual summary of the document. It may also appear elsewhere in the body of the document itself. It is highly desirable that the abstract of classified documents be unclassified. Each paragraph of the abstract shall begin with an indication of the security classification of the information in the paragraph (unless the document itself is unclassified) represented as (S), (C), or (U). It is not necessary to include here abstracts in both official languages unless the text is bilingual.)

Presented is a method to estimate the element gains and phases of a sensor array when interfering signals, including specular multipath, are present. A movable calibration source is used. The element gains are derived from the relative output powers at the array elements. The element phases are obtained by transforming the array snapshots to make the source direction appear fixed and then maximizing a function constructed with the transformed snapshots.

Computer simulations produce highly accurate estimates of element gains and phases when the signal directions are known and the signal-to-noise ratio is reasonably high. When the directions are not known, the set of element phase estimates contains an additional component which produces a bias in direction estimates.

14. KEYWORDS, DESCRIPTORS or IDENTIFIERS (technically meaningful terms or short phrases that characterize a document and could be helpful in cataloguing the document. They should be selected so that no security classification is required. Identifiers, such as equipment model designation, trade name, military project code name, geographic location may also be included. If possible keywords should be selected from a published thesaurus. e.g. Thesaurus of Engineering and Scientific Terms (TEST) and that thesaurus-identified. If it is not possible to select indexing terms which are Unclassified, the classification of each should be indicated as with the title.)

Array Calibration

Element Gains

Element Phases

Specular Multipath Interference